

DOI: 10.1002/cphc.201402307

Effect of the Cationic Surfactant Moiety on the Structure of Water Entrapped in Two Catanionic Reverse Micelles Created from Ionic Liquid-Like Surfactants

Cristian C. Villa, Juana J. Silber, N. Mariano Correa,* and R. Darío Falcone*^[a]

The behavior of water entrapped in reverse micelles (RMs) formed by two catanionic ionic liquid-like surfactants, benzyl-*n*-hexadecyldimethylammonium 1,4-bis-2-ethylhexylsulfosuccinate (AOT-BHD) and cetyltrimethylammonium 1,4-bis-2-ethylhexylsulfosuccinate (AOT-CTA), was investigated by using dynamic (DLS) and static (SLS) light scattering, FTIR, and ¹H NMR spectroscopy techniques. To the best of our knowledge, this is the first report in which AOT-CTA has been used to create RMs and encapsulate water. DLS and SLS results revealed the formation of RMs in benzene and the interaction of water with the RM interface. From FTIR and ¹H NMR spectroscopy data, a difference in the magnitude of the water–catanionic surfactant interaction at the interface is observed. For the AOT-BHD

RMs, a strong water–surfactant interaction can be invoked whereas for AOT-CTA this interaction seems to be weaker. Consequently, more water molecules interact with the interface in AOT-BHD RMs with a completely disrupted hydrogen-bond network, than in AOT-CTA RMs in which the water structure is partially preserved. We suggest that the benzyl group present in the BHD⁺ moiety in AOT-BHD is responsible for the behavior of the catanionic interface in comparison with the interface created in AOT-CTA. These results show that a simple change in the cationic component in the catanionic surfactant promotes remarkable changes in the RMs interface with interesting consequences, in particular when using the systems as nanoreactors.

1. Introduction

Reverse micelles (RMs) are supramolecular assemblies of surfactants formed in nonpolar solvents, in which the polar head groups of the surfactants point inward and the hydrocarbon chains point toward to the nonpolar medium.^[1] One of the most used surfactants with the ability to form RMs is anionic sodium 1,4-bis-2-ethylhexylsulfosuccinate (Na-AOT), which can solubilize water in a variety of nonpolar solvents.^[1] The amount of water dispersed in the organized system can be expressed by the ratio W_0 ($W_0 = [\text{Water}]/[\text{Surfactant}]$).^[1] Other surfactants used to create RMs are the cationic species benzyl-*n*-hexadecyldimethylammonium chloride (BHDC) and hexadecyltrimethylammonium bromide (CTAB). BHDC forms RMs without the addition of cosurfactants^[1–5] but CTAB needs the presence of a cosurfactant, usually an alcohol, to generate RMs.^[6–9]


It is known that mixtures of surfactants can exhibit considerable synergistic advantages in their properties and applications.^[10] Therefore, a new class of surfactant emerges: the catanionic surfactants.^[11–17] In particular, the catanionic surfactant group created when ionic surfactants are mixed in a 1:1 ratio and the counterions are totally removed is attractive^[17] because this kind of surfactant has shown the ability to form dif-

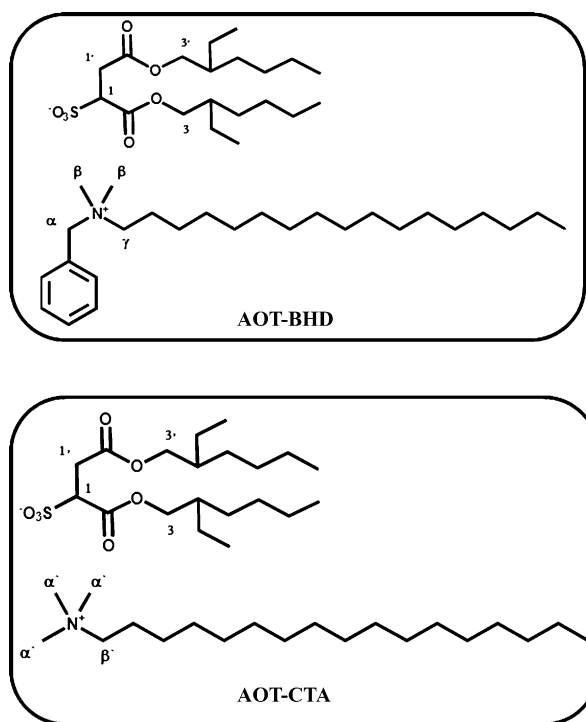
ferent organized systems, such as normal micelles and RMs,^[15,17–20] vesicles,^[15,20,21] and liquid crystals.^[20,22]

Another attractive topic is the emerging field in which ionic liquids^[23] (ILs) with amphiphilic properties are synthesized.^[24,25] In this regard,^[15] we recently reported the synthesis of a new catanionic IL-like surfactant, AOT-BHD (Scheme 1), which resulted from a mixture of Na-AOT and BHDC and showed characteristics of a room-temperature IL with amphiphilic properties. This IL-like surfactant was isolated from the original surfactant mixture (and elimination of NaCl) and showed properties absolutely different from Na-AOT and BHDC. In particular, we demonstrated that this unique surfactant can form different organized systems (RMs and vesicles) depending on the solvent used. Thus, we investigated its ability to form RMs in nonpolar solvents and spontaneous large unilamellar vesicles (LUVs) in water.^[15]

It is known that interfacial water can interact in different ways with the RM interface.^[3,26–28] Although in AOT RMs this interaction is through hydrogen bonding^[3,26,27] between the sulfonate head group and water, in BHDC RMs the interaction occurs between the quaternary ammonium and the free electron pairs of oxygen from the water.^[3,4,26] It is motivating to explore the interaction between the entrapped water and the interface formed by catanionic surfactants in RMs, in which both anionic and cationic polar head groups are present. Therefore, in this contribution we report a comparison of the amphiphilic properties and the sequestered water structure of the RMs created by AOT-BHD and a novel catanionic surfactant, AOT-CTA (see Scheme 1), which resulted from a mixture of anionic

[a] C. C. Villa, Prof. J. J. Silber, Prof. N. M. Correa, Dr. R. D. Falcone
Departamento de Química
Universidad Nacional de Río Cuarto
Agencia Postal # 3. C.P. X5804BYA Río Cuarto (Argentina)
E-mail: mcorrea@exa.unrc.edu.ar
rfalcone@exa.unrc.edu.ar

 Supporting Information for this article is available on the WWW under
<http://dx.doi.org/10.1002/cphc.201402307>



Scheme 1. Molecular structures of the catanionic surfactants AOT-BHD and AOT-CTA. Specific protons observed in NMR spectra are labeled.

Na-AOT and cationic CTAB. This new surfactant has a melting point of around 67 °C, a characteristic that allows us to classify it as an IL. In particular, we investigated the ability of both catanionic IL-like surfactants to form RMs in nonpolar solvents, and through FTIR and ^1H NMR spectroscopy techniques we studied the interaction between the entrapped water and the interface created. Our results reveal the formation of RMs in benzene and demonstrate the interaction between water and the RM interface because the droplet size increased as the amount of entrapped water was increased. Moreover, the water molecules interact differently with the interface in AOT-BHD compared with AOT-CTA RMs.

2. Results and Discussion

To evaluate whether both catanionic surfactants can be used to generate RMs, the first experiment performed was to investigate the phase diagram of the ternary system, by keeping the surfactant concentration constant and changing the amount of water to be incorporated. First, the solubility of AOT-BHD and AOT-CTA in different nonpolar solvents, such as *n*-heptane, chlorobenzene, and benzene, was tested. As reported previously,^[15] AOT-BHD is only soluble in aromatic solvents, as in the case of BHDC. Note that BHDC is a surfactant that cannot be dissolved in aliphatic hydrocarbons,^[4,5,26] but Na-AOT is perfectly soluble in both kind of solvent. In view of these facts, apparently the solubility of this catanionic surfactant is governed by the cationic surfactant moiety. However, AOT-CTA is soluble in both aliphatic (*n*-heptane) and aromatic solvents (benzene and chlorobenzene), similar to the behavior

Table 1. The maximum amount of water solubilized (W_0^{max}) in different RMs at [surfactant] = 0.1 m. $T = 35$ °C.

Solvent	W_0^{max} AOT-BHD	AOT-CTA
<i>n</i> -heptane	–[a]	1.0
benzene	1.6	2.5
chlorobenzene	1.8	3.0

[a] AOT-BHD is not soluble in *n*-heptane.

of Na-AOT. It must be noted that CTAB is insoluble in both aromatic and aliphatic solvents and thus the solubility of AOT-CTA is dominated by the anionic component, in contrast to AOT-BHD. The next step was to evaluate the amount of water that both RMs can solubilize to form clear and stable ternary mixtures. Table 1 summarizes the maximum amount of water solubilized (W_0^{max}) by different catanionic RMs at [surfactant] = 0.1 m. As can be observed, the W_0^{max} values reached for both catanionic surfactants are different; the AOT-CTA RMs are able to dissolve approximately double the amount of water that AOT-BHD RMs can in each solvent tested. This result suggests that the interfacial composition and the natural curvature in both RMs are different. Additionally, for example, in benzene the W_0^{max} values observed in both catanionic RMs are smaller than for Na-AOT ($W_0^{\text{max}} \approx 15$) or BHDC RMs ($W_0^{\text{max}} \approx 25$).^[2–4] Results also show that the chemical structure of both catanionic surfactants (see Scheme 1) has a dramatic effect on the behavior as a surfactant in comparison with the amphiphilic precursors.

To evaluate the formation of RMs and to compare the results obtained for both catanionic surfactants, we decided to use only benzene as the nonpolar solvent. Thus, the systems formed by benzene/AOT-BHD/water and benzene/AOT-CTA/water were studied.

2.1 DLS and SLS Experiments

To evaluate the formation of the catanionic RMs and to discard the presence of bicontinuous structureless microemulsions,^[1] the systems formed by using AOT-BHD and AOT-CTA were studied by using the DLS technique. When new reversed micellar systems are explored, a crucial question has to be answered: is the water effectively entrapped by the surfactant to create a true RM in the organic solvent or is the water dissolved only in the organic solvent/surfactant mixture without any molecular organization?^[1,28] DLS can be used to answer this question because if water is really encapsulated to form RMs through interactions with the interface, the droplet size must increase as the W_0 value increases with a linear tendency (swelling law of RMs), as established for other RMs.^[4,29] This feature would also show that the benzene/catanionic surfactant/water system consists of discrete spherical and noninteracting droplets of water stabilized by the surfactant layer.

Herein, all DLS experiments were carried out at a fixed surfactant concentration (0.02 m) and interdroplet interactions have been neglected.^[30] Thus, it is appropriate to introduce an

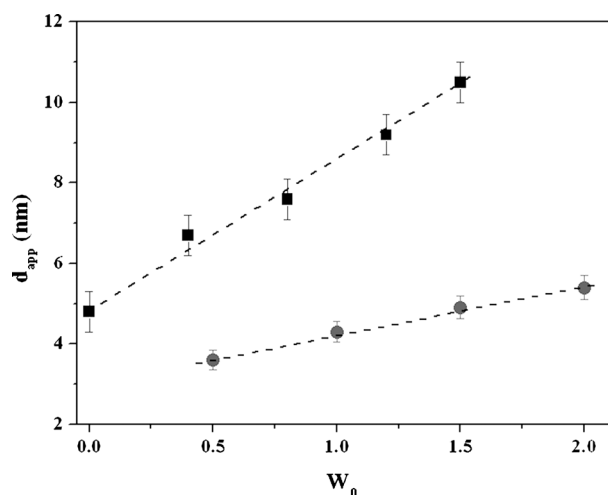


Figure 1. Apparent diameter (d_{app}) values of the benzene/AOT-BHD/water RMs (■) and benzene/AOT-CTA/water RMs (●) obtained at 35 °C at various W_0 values. [Surfactant] = 0.02 M. The straight lines are guides for the eye.

apparent hydrodynamic diameter (d_{app}) so that the systems studied herein can be compared with previous studies.^[4,31] In Figure 1, d_{app} values for RMs studied at different W_0 values for both cationic surfactants are shown. It can be seen that there is an increase in the droplet size when the water content was increased in both systems, which shows that the water was entrapped by the surfactant layer to form RMs. Also, the linear tendency of the droplet size is observed in both systems across the whole range of W_0 studied. The linear tendency observed for both RMs indicates that the droplets are not interacting and are probably spherical.

It is interesting to note that although both systems show a linear tendency, the droplet sizes at fixed W_0 are quite different. For example, at $W_0 = 1.5$ the d_{app} value is around 10.5 nm for AOT-BHD RMs and around 4.9 nm for AOT-CTA RMs. Moreover, the d_{app} values obtained for AOT-BHD in benzene are larger than the corresponding values reported for Na-AOT and BHDC in the same organic solvent.^[4,32–34] Unfortunately, neither Na-AOT nor BHDC have droplet sizes reported in benzene within the same W_0 range as our cationic surfactants. However, there is a significant point to note in that the droplet sizes for comparable RMs, such as toluene/Na-AOT/water^[32] and benzene/BHDC/water RMs^[4] at $W_0 = 10$ are around 5 and 8.3 nm, respectively, which are both notably smaller than for benzene/AOT-BHD/water RMs even at higher water contents. A similar situation occurs with the droplet size of AOT-CTA RMs, for which the d_{app} value obtained for AOT-CTA RMs at $W_0 = 1$ (4.3 nm) is comparable to the droplet sizes reported for toluene/Na-AOT/water at $W_0 = 10$.^[32] As mentioned before, the surfactant CTAB is not able to form RMs in the absence of a cosurfactant and for this reason cannot be compared with the AOT-CTA RMs sizes. Prior to explaining these results, it is important to consider that the RM droplet size depends, among many other variables, on the effective packing parameter of the surfactants (p), defined as $p = v/a l_c$ in which v and l_c are the volume and the length of the hydrocarbon chain, respectively, and a is the surfactant head group area.^[33] The RM sizes are

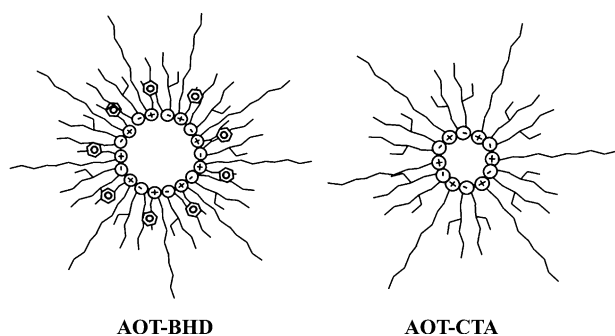
larger when the surfactant packing parameter values are smaller.^[35,36] Thus, all the factors that decrease the v values and/or increase a values decrease the packing parameter. It has been shown by using DLS that the polar solvent–surfactant interactions in Na-AOT^[1,28,29,37,38] and BHDC RMs^[4,37,38] are key for RM droplet size control. For example, when an encapsulated polar solvent interacts strongly with the surfactant polar head group, the a value of the surfactant is increased with a consequent decrease in the surfactant–packing parameter and an increase in the RM droplet size.^[1,29]

Considering our DLS results, two facts have to be explained: 1) the differences in the droplet sizes of the cationic RMs in comparison with the values reported for the precursor surfactants and 2) the differences in the droplet size between both cationic RMs.

The ionic nature of the polar head group of the precursor surfactants (Na-AOT, BHDC, and CTAB) and the requirement to act as counterions for each other in the cationic surfactants can produce a known change in the p parameter compared with the precursors. We hypothesize that this change in the p value is attributed to an increment in the effective area of the cationic surfactant. AOT-BHD and AOT-CTA present larger interfacial areas than the anionic and the cationic moiety separately and thus the packing parameter decreases and the droplet size increases. Moreover, by taking into account the fact that the cationic components in both cationic surfactants have practically the same length of hydrocarbon chain (l_c), we think that the main differences between the p parameters can be attributed to the v/a ratio. In AOT-BHD, it is possible that the benzyl group is located near to the quaternary nitrogen of BHD⁺, which increases the effective area in comparison with AOT-CTA. This increment in a would decrease v/a , which would decrease the p parameter and increase the droplet size.

However, the different slopes in the droplet size plots in Figure 1 could indicate a different water–surfactant interaction in both cationic systems. Thus, the small droplet sizes obtained for water entrapped in AOT-CTA RMs compared with the values obtained for AOT-BHD RMs can be explained by considering a weaker water–surfactant interaction present at the RM interface. The weak interaction with the cationic interface in benzene/AOT-CTA/water RMs results in a slight increase in area a and droplet size with increasing the W_0 value. In contrast, when AOT-BHD is used as surfactant, water can apparently interact strongly with the surfactant, which increases the effective area a (consequently, the p parameter is decreased) and d_{app} values increase. Thus, a simple change in the cationic component in the cationic surfactant promotes remarkable changes in the RM interface. If a spherical shape and an intercalated distribution of the surfactant moieties are assumed, the cationic surfactant distribution at the interface can be represented as shown in Scheme 2, which creates a new interface with unexplored physicochemical properties.

To support the prediction of the shape from the DLS study, the SLS technique was used. The aggregation numbers (N_{agg}) of the systems at equal W_0 values were determined and the values are listed in Table 2. As can be seen, at $W_0 = 1.5$ AOT-BHD RMs present a N_{agg} value of around 36, which for AOT-



Scheme 2. Schematic representation of AOT-BHD and AOT-CTA surfactant distribution in the reverse micelle system.

Table 2. Aggregation numbers (N_{agg}) for benzene/AOT-BHD/water and benzene/AOT-CTA/water RMs calculated using the SLS technique. $T=35^\circ\text{C}$, $W_0=1.5$.

RMs	d_{app} [nm] ^[a]	N_{agg}
benzene/AOT-BHD/water	10.5	36 ± 5
benzene/AOT-CTA/water	4.9	29 ± 5

[a] Data from Figure 1.

CTA RMs indicates around 29 cationic surfactant molecules per micelle. If these data are compared with the N_{agg} values reported for the surfactant precursors,^[39,40] these values are smaller but it must be noted that one cationic surfactant molecule is comprised of two amphiphilic moieties and the water encapsulated is much smaller in the cationic RMs. Considering this, the N_{agg} values for both cationic RMs suggest that the shape of these RMs can be considered to be practically spherical (see Scheme 2), as was assumed from the DLS experiments. However, because there is no significant difference between the N_{agg} values of both cationic RMs, we assume that the variation in the d_{app} values of both systems (Figure 1) cannot be attributed to the number of molecules that form the RMs but to the different water–surfactant interaction at the interface, as suggested by the DLS data.

2.2 FTIR Experiments

To acquire a full panorama for these cationic RMs, we chose to monitor the microenvironment that the water and both surfactant molecules experience inside AOT-BHD and AOT-CTA RMs. Thus, we first focused on the O–D stretching mode of the entrapped water molecules and then on the asymmetric S=O and carbonyl stretching modes from the AOT moiety. The results were compared with the stretching vibration modes of Na-AOT.

2.2.1 O–D Stretching Band ($\nu_{\text{O-D}}$)

It is known that water exhibits a broad band in the 3500–3200 cm^{-1} region, which is assigned to the O–H stretching.^[41] In the liquid phase, this band not only corresponds to the O–H

stretching but also to the vibrational coupling of the H–O–H bonds.^[42,43] This phenomenon is also observed for deuterated water (D_2O), for which the band recorded in the 2570–2350 cm^{-1} region, also broad, corresponds to the O–D stretching mode and the vibrational couplings of the D–O–D bonds. In our FTIR studies we decided to use monodeuterated water (HDO), which exhibits a narrow band at around 2570–2350 cm^{-1} that can be assigned only to the O–D stretching band ($\nu_{\text{O-D}}$).^[43,44] This methodology has been used previously for aqueous AOT RMs to avoid the vibrational coupling and simplify the data analysis.^[44,45]

Figure S1 in the Supporting Information displays the FTIR spectra of HDO entrapped in AOT-BHD RMs (Figure S1A) and AOT-CTA (Figure S1B) at different W_0 values in the region of 2640–2420 cm^{-1} . Figure 2 shows the shifts in the $\nu_{\text{O-D}}$ values

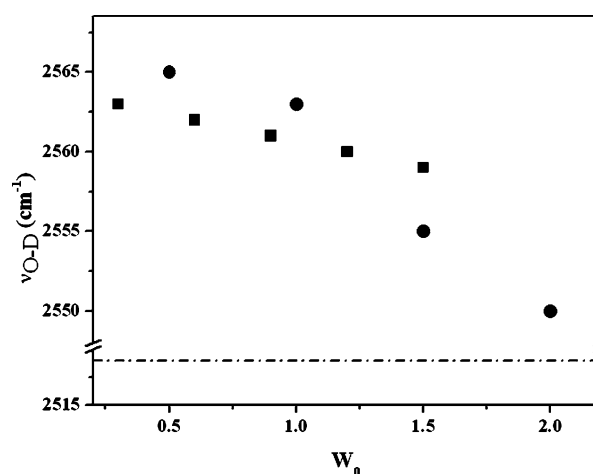


Figure 2. Shifts in the O–D stretching band ($\nu_{\text{O-D}}$) with increasing W_0 values for the benzene/AOT-BHD/HDO RMs (■) and benzene/AOT-CTA/HDO RMs (●). The corresponding value for neat HDO (---) is included as a reference.

for HDO in the AOT-BHD and AOT-CTA RMs. From Figure 2, two facts can be observed: 1) all the O–D stretching frequencies in both cationic RMs are larger than the corresponding value for neat HDO (2519 cm^{-1})^[46] and 2) the trend of the changes in the $\nu_{\text{O-D}}$ values is different for both cationic RMs.

The fact that the entrapped water in AOT-BHD and AOT-CTA RMs presents $\nu_{\text{O-D}}$ values larger than neat water suggests that the water molecules are interacting with the surfactant interface and breaking its hydrogen-bond structure. It is interesting to compare the variation observed with similar studies for the RMs formed by the precursor surfactants, Na-AOT and BHDC, because CTAB does not form RMs as was previously discussed. Figure S2 shows the shifts of the $\nu_{\text{O-D}}$ values for HDO entrapped in benzene/Na-AOT and benzene/BHDC RMs. Note that the behavior in Na-AOT RMs is opposite to that observed for BHDC RMs. In benzene/Na-AOT/HDO RMs, the hydrogen-bond interaction between the entrapped water and the AOT polar head group at the interface disrupt the hydrogen-bond network of water.^[43–45] In contrast, for water entrapped in benzene/BHDC RMs we observed that $\nu_{\text{O-D}}$ values appear at lower frequencies than neat water. This fact was explained by consid-

ering that in BHDC RMs the cationic polar head group is solvated by ion–dipole interactions through the nonbonding electrons pairs of oxygen, which leads to a smaller force constant in the O–H bond.^[41] Thus, taking into account these backgrounds, our results indicate that the water–catanionic surfactant interaction in AOT-BHD and AOT-CTA RMs is mainly due to hydrogen bonding.

Additionally, Figure 2 also shows that although for both catanionic RMs the $\nu_{\text{O-D}}$ values shift to lower frequencies as the W_0 value increased, the changes in magnitude are different. For example, in AOT-BHD RMs the frequency of the O–D band changed from 2563 cm^{-1} at $W_0=0.3$ up to 2559 cm^{-1} at $W_0=1.5$ (only 4 cm^{-1}), whereas in AOT-CTA RMs the $\nu_{\text{O-D}}$ value was 2565 cm^{-1} at $W_0=0.5$ and the band shifted to 2550 cm^{-1} at $W_0=2$, which shows a shift of 15 cm^{-1} . These results suggest a difference in the magnitude of the water–catanionic surfactant interaction at the interface, an observation that also was inferred from the DLS data. Even though we observed hydrogen-bond interactions for both catanionic surfactants, the strength of this seems to be different. For the AOT-BHD RMs a stronger water–surfactant interaction can be invoked whereas for AOT-CTA this interaction seems to be weaker. This would lead to more water molecules interacting with the interface in AOT-BHD RMs (with its hydrogen-bond network disrupted), which produces a smaller change in the $\nu_{\text{O-D}}$ value over the whole W_0 range studied. Conversely, for AOT-CTA RMs a weaker water–catanionic surfactant interaction allows the water molecules to establish hydrogen bonds with each other and produce a larger shift in the $\nu_{\text{O-D}}$ values.

2.2.2 AOT Carbonyl Stretching Band ($\nu_{\text{C=O}}$)

The carbonyl stretching band ($\nu_{\text{C=O}}$) of Na-AOT has been widely studied in both the solid state^[43] and RMs.^[47–51] It appears as a broad band with a peak around 1735 cm^{-1} and a shoulder around 1724 cm^{-1} . The explanations given for the Na-AOT C=O band shape are quite confusing and the causes of its asymmetry are not clear. Three different interpretations can be found in the literature but none of them are conclusive.^[51] The first explanation claims that this band arises from a mixture of the AOT predominant rotational isomers, in particular the *gauche* ($\nu_{\text{C=O}}$ around 1720 cm^{-1}) and *trans* ($\nu_{\text{C=O}}$ around 1730 cm^{-1} ; see Scheme S2).^[51a] The ratio of the conformers should vary with the nature of the microenvironment. In polar media, the *gauche*-like conformer is expected to be favored because in this conformation the whole polar group remains directly pointed toward the polar side of the RM interface. Conversely, in apolar media the *trans*-like rotamer is favored because a carbonyl group vicinal to the SO_3^- group moves from the polar side to the apolar region of the interface.^[50] However, when polar solvents are encapsulated inside Na-AOT RMs,^[1,50] the 1720 cm^{-1} band does not decrease as expected for a rotamer equilibrium shift. Consequently, it seems that other effects are affecting the AOT C=O asymmetric band.^[47, 51b] The second possible explanation arises from considering that AOT has two C=O groups that are not symmetrically equivalent, which will give rise to two bands even in the

absence of rotational isomerism.^[43] The third possible explanation for the Na-AOT C=O band can be attributed to the presence of the Na^+ counterion near to one of the carbonyl groups that promotes asymmetry in the C=O band. Moran et al.^[47] suggested a weak interaction between the cation and the carbonyl groups that could affect the intensity of the shoulder at around 1724 cm^{-1} . Thus, when the surfactant is forming RMs, the intensity of the shoulder could diminish in comparison with the band observed in the solid state, which reflects that Na^+ is closer to C=O in the solid state than in solution. However, until now no data for replacing the counterions of AOT were strong enough to make a conclusion about this behavior. For example, it is known that Na^+ was replaced by other alkali metals,^[51b] but to the best of our knowledge there was no clear impact on the carbonyl group.

Figure 3 shows the FTIR spectra that correspond to the carbonyl stretching band for Na-AOT, AOT-BHD, and AOT-CTA surfactants dissolved in benzene at $W_0=0$. It is possible to see

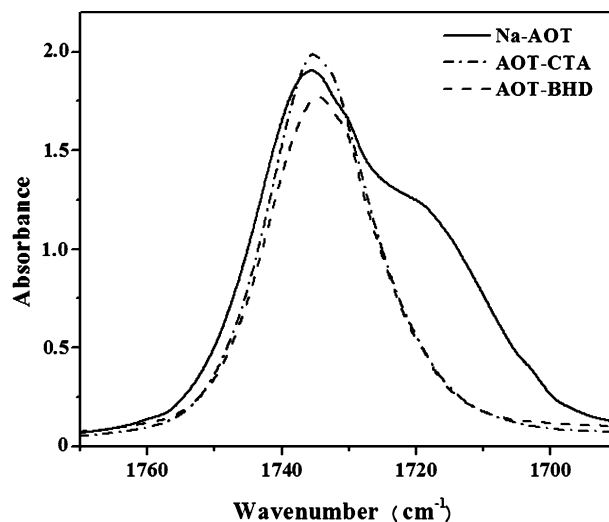


Figure 3. FTIR spectra of Na-AOT/benzene, AOT-BHD/benzene and AOT-CTA/benzene RMs at $W_0=0$ in the region of 1690–1770 cm^{-1} ($\nu_{\text{C=O}}$). The benzene bands have been subtracted. [Surfactant] = 0.05 m.

that the C=O band shows a notable difference in its shape for both catanionic surfactants in comparison with that observed for Na-AOT. As discussed above, in Na-AOT the C=O band appears as broad band with a main peak at 1735 cm^{-1} and a shoulder around 1724 cm^{-1} , whereas in both catanionic surfactants it appears as a symmetrical band with a peak around 1735–1734 cm^{-1} . These results suggest that the replacement of Na^+ by another large cation with different structure has an impact on the shape of the $\nu_{\text{C=O}}$ band. Thus, the presence of cations such as BHD^+ or CTA^+ , which both have amphiphilic properties, result in the cations being located further from the AOT polar head group than the Na^+ location. This different location of the cations promotes a symmetrical C=O band and reinforced the idea that Na^+ being located near to the C=O group could be the reason for the asymmetry observed in the AOT band.

Figures S3A and S3B show plots of the FTIR spectra of water entrapped in AOT-CTA and AOT-BHD RMs in the region of C=O stretching mode for different amounts of water. As shown in Figure S3A, the C=O stretching band for the benzene/AOT-CTA/water RMs did not show any significant change in position, shape, or absorbance as the value of W_0 was increased. The same tendency was observed for the benzene/AOT-BHD/water system (Figure S3B), in which the $\nu_{\text{C=O}}$ value maintained a constant position at 1735 cm^{-1} as the W_0 value was increased. It is known that many factors can influence the position of the C=O band, including hydrogen-bond formation and ionic interactions, which lead to displacement of the band to lower frequencies.^[43] Additionally, the hydrogen-bond interaction not only induces a shift in the band but can produce a marked effect on its intensity. The absorption coefficient of the band increases by multiple units when the carbonyl group forms hydrogen bonds. Durantini et al.^[50] found that in *n*-heptane/Na-AOT/ethylene glycol and *n*-heptane/Na-AOT/propylene glycol RMs, both polar solvents not only interact strongly with the sulfonate group but also penetrate the micelle interface enough to interact through hydrogen bonding with the carbonyl groups of the surfactant. This interaction is reflected in a large increase in the intensity of the C=O band. As shown in Figure S3, the lack of absorption changes in the stretching band of carbonyl group of the AOT moiety in both AOT-BHD and AOT-CTA RMs indicates that the entrapped water does not penetrate the interface enough to interact through hydrogen bonds with the carbonyl groups of AOT.

2.2.3 AOT Sulfonate Asymmetric Stretching Band ($\nu_{\text{a}}\text{SO}_3$)

The AOT surfactant presents two sulfonate stretching vibration modes that are interesting to investigate: the asymmetric S=O stretching band (around $1130\text{--}1330\text{ cm}^{-1}$) and the symmetric S=O stretching mode (around 1050 cm^{-1}).^[50] However, because of the strong in-plane C–H bending mode of benzene (around $1060\text{--}1020\text{ cm}^{-1}$), the symmetric S=O stretching mode cannot be observed in RMs prepared in this solvent. Moreover, because the asymmetric S=O stretching vibration band is very sensitive to both hydrogen-bond interactions between the water and the SO_3^- group of Na-AOT and the electrostatic interaction between the Na^+ counterion and the SO_3^- group,^[1,43–45,47–49,51b,52,53] we decided to explore this region to obtain more information about the different water–catanionic polar head interactions.

The FTIR band assigned to the asymmetric stretching mode of the sulfonate group ($\nu_{\text{a}}\text{SO}_3$) appears as a weak doublet at about 1214 and 1242 cm^{-1} in solid Na-AOT, which has been attributed to the lifting of the degeneracy of this vibration by an asymmetric interaction between the Na^+ and the sulfonate head group.^[51b] The magnitude of the splitting, defined as $\Delta\nu_{\text{a}}\text{SO}_3$, is indicative of the strength of the perturbation of the SO_3^- by the cation, and is larger when the ionic interaction is stronger.^[47] In RMs, the band shows a doublet at 1255 and 1213 cm^{-1} at $W_0=0$ and the $\Delta\nu_{\text{a}}\text{SO}_3^-$ value increases from 28 cm^{-1} in solid Na-AOT to 42 cm^{-1} in the benzene RMs, which reflects an increase in the strength in the interaction between

Na^+ and SO_3^- .^[43,47,50] In the presence of entrapped water, it was shown that the magnitude of the $\Delta\nu_{\text{a}}\text{SO}_3$ value decreases with increasing micelle hydration due to a weakening of the sodium–sulfonate interaction after hydrogen-bond interactions between water and the AOT polar head group with a corresponding increase in their spatial separation.^[43]

Figure 4 shows the FTIR spectra of Na-AOT, AOT-BHD, and AOT-CTA in benzene at $W_0=0$ in the region of the asymmetric stretching mode of SO_3^- . It can be seen that the splitting of

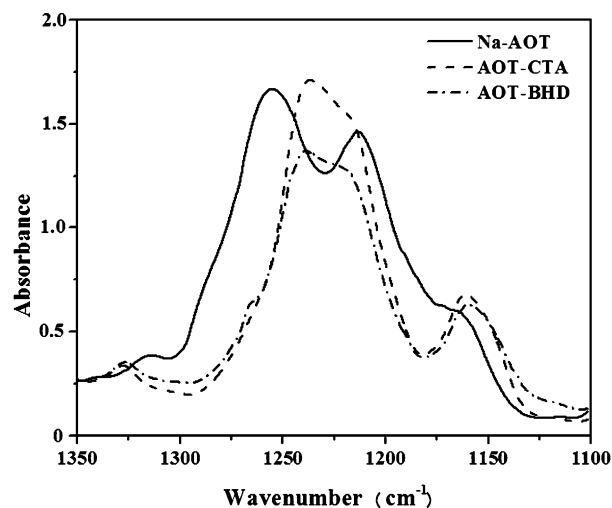


Figure 4. FTIR spectra of Na-AOT/benzene, AOT-BHD/benzene, and AOT-CTA/benzene RMs at $W_0=0$ in the region of $1350\text{--}1100\text{ cm}^{-1}$ ($\nu_{\text{a}}\text{SO}_3$). The benzene bands have been subtracted. [Surfactant] = 0.05 m .

the two peaks of $\nu_{\text{a}}\text{SO}_3$ decreases considerably in both catanionic surfactants, which indicates a weaker interaction between the sulfonate group and the new counterions. This weak interaction can be attributed to the spatial separation between both components of the catanionic surfactants, due to the steric effect around their polar head groups and the amphiphilic character of the components.

Figure 5 shows typical FTIR spectra of water entrapped in benzene/AOT-CTA RMs at different W_0 values in the region of 1330 to 1100 cm^{-1} , which corresponds to the $\nu_{\text{a}}\text{SO}_3$ band, are reported. Spectra obtained for benzene/AOT-BHD/water RMs are presented in Figure S4 (see the SI). From Figures 5 and S4 it is possible to observe that the splitting of the two intense peaks in both catanionic RMs did not show any significant change in position, shape, or absorbance as the water content increased. Moreover, in both cases the magnitude of the splitting of the main peaks remained practically constant as the W_0 value was increased. These results are very different from those obtained for water entrapped in benzene/Na-AOT,^[48,50,51b] in which the magnitude of the $\Delta\nu_{\text{a}}\text{SO}_3$ values decreases as a consequence of the interaction between the water molecules and the surfactant polar head group at the interface.

In our case, the absence of variation in the asymmetric sulfonate band suggests that water molecules do not disrupt the interaction between the SO_3^- and BHD^+ or CTA^+ . As men-

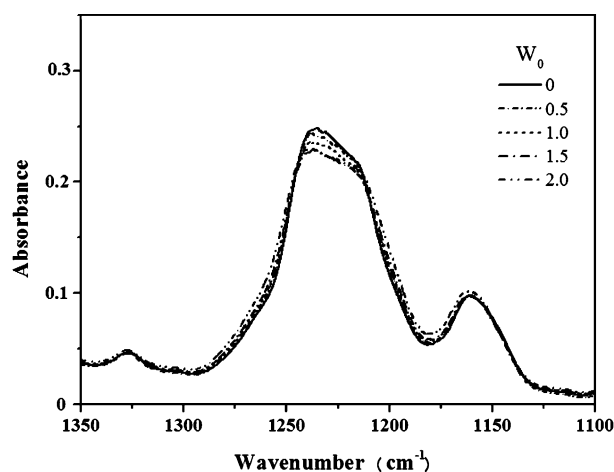


Figure 5. FTIR spectra of benzene/AOT-CTA/water RMs at different W_0 values in the region of 1330–1100 cm^{-1} ($\nu_s\text{SO}_3$). The benzene bands have been subtracted. [AOT-CTA] = 0.05 M.

tioned for $W_0=0$, in both catanionic RMs there is already a weak interaction between the AOT sulfonate and the counterions because both ions (SO_3^- -BHD $^+$ or SO_3^- -CTA $^+$) are more distant from each other than in Na-AOT. This causes the asymmetric sulfonate band to be insensitive to changes when water is added. However, this fact cannot be interpreted as an absence of water interaction with the polar head groups. The study of the O–D band indicated that in both AOT-BHD and AOT-CTA RMs the entrapped water interacts (with different magnitude) with the interface but, due to the change in the component of the surfactant, the asymmetric sulfonate stretching band cannot be used as a water-addition sensor.

2.3 ^1H NMR Spectroscopy Experiments

Figure 6 displays typical ^1H NMR spectra for water entrapped in benzene/AOT-BHD RMs at different W_0 values in the region of $\delta=3$ to 5 ppm. Figure S5 shows the ^1H NMR spectra that correspond to the benzene/AOT-CTA/water system. As can be observed from both figures, several signals can be monitored. In this sense, different protons were investigated and first we present the results obtained by sensing the H of the entrapped water and then the protons nearest to the polar head groups in AOT-BHD and AOT-CTA surfactants (protons 1, 1', 3, 3', α , β , and γ of AOT-BHD and 1, 1', 3, 3', α' , and β' of AOT-CTA in Scheme 1).

2.3.1 The Protons of Water

Figure 7 shows data corresponding to the chemical shift of H (from water) in AOT-BHD and AOT-CTA RMs at different water contents. It can be seen that the proton signal shifts upfield when W_0 is increased in both systems, however, the magnitude of the shift is different for both RMs investigated. For example, in benzene/AOT-BHD/water the proton signal changes from $\delta=3.36$ ppm at $W_0=0.4$ to $\delta=3.51$ at $W_0=1.5$. In AOT-CTA RMs, the proton from water molecules appears at $\delta=$

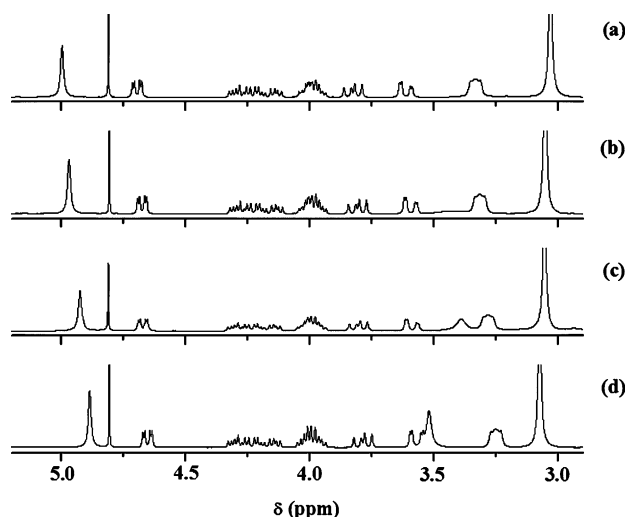


Figure 6. ^1H NMR spectra for benzene/AOT-BHD/water RMs at different W_0 values: a) 0, b) 0.4, c) 0.8, d) 1.2. [AOT-BHD] = 0.05 M.

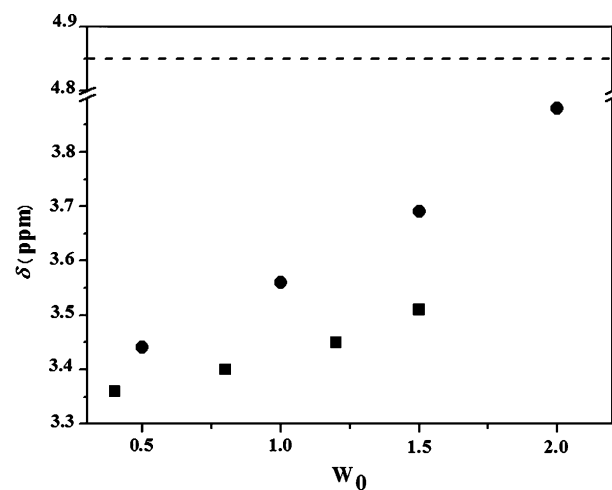


Figure 7. ^1H NMR chemical shifts of H (from water) in benzene/AOT-BHD/water (\blacksquare) and benzene/AOT-CTA/water (\bullet) RMs at different W_0 values. [surfactant] = 0.05 M. The corresponding value for neat water^[54] ($\delta=4.85$ ppm) is included for comparison.

3.44 ppm at $W_0=0.5$ and $\delta=3.88$ ppm at $W_0=2.0$. Moreover, in AOT-BHD RMs the signal appears substantially further downfield compared with the value observed for AOT-CTA RMs. For example, at $W_0=1.5$ the proton signal appears almost $\delta=0.4$ ppm downfield in AOT-BHD RMs compared with AOT-CTA RMs. It should be noted that the value of H for neat water^[54] ($\delta=4.85$ ppm) was not achieved for any of the catanionic RMs (see straight line in Figure 7).

Similar behavior was observed by Heatley^[54] in cyclohexane/Na-AOT/water RMs and also by Stahla et al.^[55] for the benzene/Na-AOT/water system. In both cases the upfield shift of the proton signal (from water) in comparison with neat water was attributed to disruption of the hydrogen-bond structure of entrapped water due to its interaction with the surfactant. With an increased amount of water within the RMs, the entrapped

water begins to recover the hydrogen-bond structure of neat water. A stronger interaction between the entrapped water and the interface leads to fewer water molecules interacting with each other and consequently a more upfield shift in the proton signal. As explained before in our study of the changes in the O–D stretching band in both catanionic surfactants, the interaction of the entrapped water and the interface disrupt its hydrogen-bond structure and makes the $\nu_{\text{O-D}}$ values appear at higher frequencies than neat water (see Figure 2). This interaction also leads to the upfield shift in the protons signals of the water molecules in both catanionic systems.

It is also significant to note the difference in the magnitude of the downfield shift of the proton signals as the W_0 value increases. As shown in Figure 7, the shift is smaller in the AOT-BHD RMs than in the AOT-CTA RMs. Although in the AOT-BHD systems the H signal from water shifts by around $\delta=0.1$ ppm across the whole W_0 range studied, in the AOT-CTA system this shift is around $\delta=0.5$ ppm. These results agree with those obtained from FTIR spectra of the entrapped water (Figure 2), in which we observed that in the AOT-CTA RMs the O–D band has a larger shift to lower frequency than in the AOT-BHD RMs. Both studies and the DLS experiments seem to indicate that the entrapped water interacts more strongly with the interface in AOT-BHD than in the AOT-CTA system, and consequently stronger water–water interactions are observed in the latter system.

2.3.2 The Protons of the Surfactant

The protons of the surfactant also can be used as a probe to study the microenvironment created in these RMs.^[2,37,38,54–56] To present our results more clearly, we first introduce and discuss the data at $W_0=0$ and later vary the water content. Figures 6 and S5 show the ^1H NMR spectra collected for benzene/AOT-BHD and benzene/AOT-CTA RMs at $W_0=0$ in the region of the surfactant's head group, specifically protons 1, 1', 3, 3', α , β , and γ of AOT-BHD (Figure 6) and 1, 1', 3, 3', α' , and β' of AOT-CTA (Figure S5). In both cases the expected signals for the AOT anion (protons 1, 1', 3, and 3') and the cationic components (protons α , β , and γ of AOT-BHD; α' and β' of AOT-CTA) can be assigned and the chemical shifts of these protons in AOT-BHD and AOT-CTA RMs are shown in Table 3. As can be seen, the signal assigned to the H1 AOT polar head group in the AOT-BHD and AOT-CTA RMs is shifted upfield from its respective value in the Na-AOT surfactant. Protons H3 and H3' appear almost constant in both surfactants and only the H1' signal appears downfield in comparison with Na-AOT. Stahla et al.^[55] studied the ^1H NMR signals assigned to the anion AOT polar head with different metal counterions. They observed that as the counterion size was increased, the signals of the protons nearest to the sulfonate group shifted upfield as a consequence of a reduction in the interaction between the metal and the anionic moiety. These results agree with our study of the asymmetric SO_3 band, in which we observed that the interaction between the anion AOT and the CTA^+ or BHD^+ cations was weaker than Na^+ and AOT.

Table 3. ^1H NMR chemical shifts for the protons nearest to the polar head groups in Na-AOT, BHDC, AOT-BHD, and AOT-CTA RMs at $W_0=0$. [Surfactant] = 0.05 M.

	H	δ [ppm] AOT-BHD ^[a]	AOT-CTA ^[a]	Na-AOT ^[b]	BHDC ^[c]
AOT	H1	4.69	4.59	4.75	–
	H3	4.23	4.25	4.25	–
	H3'	3.98	4.00	4.07	–
BHD	H1'	3.61	3.71	3.50	–
	H α	4.99	–	–	5.42
	H β	3.02	–	–	3.51
CTA	H γ	3.32	–	–	4.07
	H α'	–	3.38	–	–
	H β'	–	3.26	–	–

[a] The labels for the H atoms in the surfactant are shown in Scheme 1.

[b] Values obtained in chlorobenzene from reference [37]. [c] Values obtained in $[\text{D}_6]$ benzene from reference [56].

The ^1H signals assigned to the protons nearest to the cationic components in both RMs also appears altered by the counterion replacement. For example, in AOT-BHD at $W_0=0$, the H α , H β , and H γ shift upfield when the catanionic surfactant forms RMs in comparison with BHDC RMs.^[56] Unfortunately, because the CTAB surfactant is not able to form RMs in the absence of a cosurfactant, it is not possible to compare the data with the AOT-CTA RMs results.

When water was added to both catanionic RMs, the proton signals values corresponding to the anionic and cationic polar head group moieties showed different behavior. Figures S6 and S7 show the chemical shifts of the protons associated with the AOT anion in the AOT-BHD and AOT-CTA RMs at various water contents. As can be observed in Figure S6, none of the signals assigned to the protons on the polar head of the anion AOT in AOT-BHD showed any shift across the whole W_0 range evaluated. Thus, the signals assigned to H1, H3', and H1 remained constant at $\delta=4.68$, 3.98, and 3.61 ppm, respectively. This same behavior was observed in the AOT-CTA RMs (Figure S7), in which all the proton signals assigned to the AOT anion remained constant at $\delta=4.59$, 4.00, and 3.71 for H1, H3', and H1', respectively. The behavior of the protons corresponding to the polar head group of Na-AOT has been explored previously. For example, Heatley^[54] reported that in the $\text{C}_6\text{D}_6/\text{Na-AOT}/\text{water}$ systems only the signal assigned to the H1 proton showed a significant shift as the W_0 value was increased. For example, the H1 signal shifted from $\delta=4.86$ ppm at $W_0=1.0$ to $\delta=4.62$ ppm at $W_0=11.7$, whereas H1' shifted from $\delta=3.64$ to 3.53 ppm across the same range of W_0 . The other two H signals remained constant with the addition of water. This behavior was attributed to the increasing spatial separation between anion AOT and its counterion, which occurs as a consequence of the hydrogen-bond interaction between the sulfonate group and the entrapped water. We already explained that there is a weaker interaction between AOT and the cationic surfactants in both AOT-BHD and AOT-CTA than that observed for AOT and sodium. This weaker interaction is probably because of the spatial separation caused by the steric effect between the polar head groups of both components. Thus, be-

cause both BHD^+ and CTA^+ are fairly separated from the AOT head group at $W_0=0$, the protons nearest to the anionic polar head moiety become insensitive to the addition of water.

Figure 8 shows the ^1H NMR chemical shift of the $\text{H}\alpha$ (see Scheme 1) signal for BHD^+ cation in the AOT-BHD RMs, studied at different W_0 values. Figure S8 shows the ^1H NMR chemical

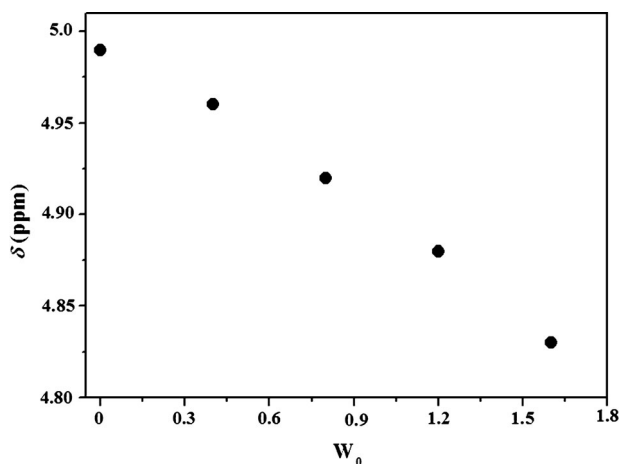


Figure 8. ^1H NMR chemical shifts of $\text{H}\alpha$ in benzene/AOT-BHD/water RMs at different W_0 values. [AOT-BHD] = 0.05 M.

shifts of $\text{H}\beta$ and $\text{H}\gamma$ for the same experiment. The peak positions of $\text{H}\alpha$ showed an upfield shift as W_0 was increased, moving from $\delta=4.99$ ppm at $W_0=0$ to $\delta=4.82$ ppm at $W_0=1.6$. However, the other protons associated with the polar head group of the BHD cation ($\text{H}\beta$ and $\text{H}\gamma$) did not show any sensitivity to the W_0 increase (Figure S8). Thus, for $\text{H}\beta$ the signal remained constant at $\delta=3.03$ ppm as W_0 was increased, whereas for $\text{H}\gamma$ the value obtained was $\delta=3.33$ ppm across the W_0 range studied. McNeil et al.^[2] studied the proton signals of the polar head of BHDC in benzene/BHDC/water RMs with increasing W_0 . They found that the $\text{H}\alpha$ signal was the most sensitive to the presence of water in the RMs and shifted upfield as W_0 was increased.^[2] This behavior was attributed to a change in the electron-withdrawing ability of the phenyl group as a result of hydration of the polar head of the surfactant. Conversely, the signals assigned to $\text{H}\beta$ and $\text{H}\gamma$ were only sensitive to the presence of water at $W_0 > 10$, once the polar head was fully hydrated. In our case, the upfield shift in the $\text{H}\alpha$ signal observed for AOT-BHD RMs could be attributed to water interacting with BHD^+ and the insensitivity of $\text{H}\beta$ and $\text{H}\gamma$ could be due to the very low water hydration level reached by the catanionic RMs. As we have explained before for the AOT-BHD RMs, the hydrogen-bond structure of the entrapped water is disrupted due to the interaction with the interface. The results obtained for the $\text{H}\alpha$ signal seem to indicate that BHD^+ also interacts with the entrapped water. We hypothesize that the benzyl group present in the BHD^+ moiety in AOT-BHD interface can produce these particular results by altering the interactions with the anionic component and with the entrapped water (see Scheme 3A).

When the ^1H NMR chemical shift of the protons nearest to the polar head group of CTA^+ (see Scheme 1) in AOT-CTA RMs were analyzed, different results in comparison with BHD^+ were obtained. Figure 9 shows the ^1H NMR chemical shifts of $\text{H}\alpha'$ and $\text{H}\beta'$ in AOT-CTA RMs, studied at different W_0 values. In this case, neither of the polar head protons of the cationic compo-

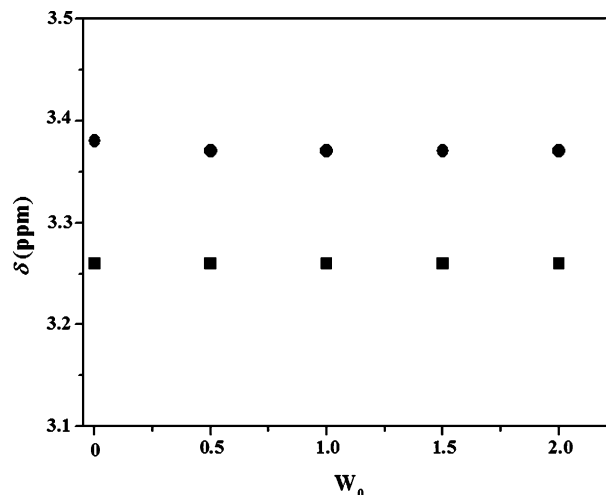
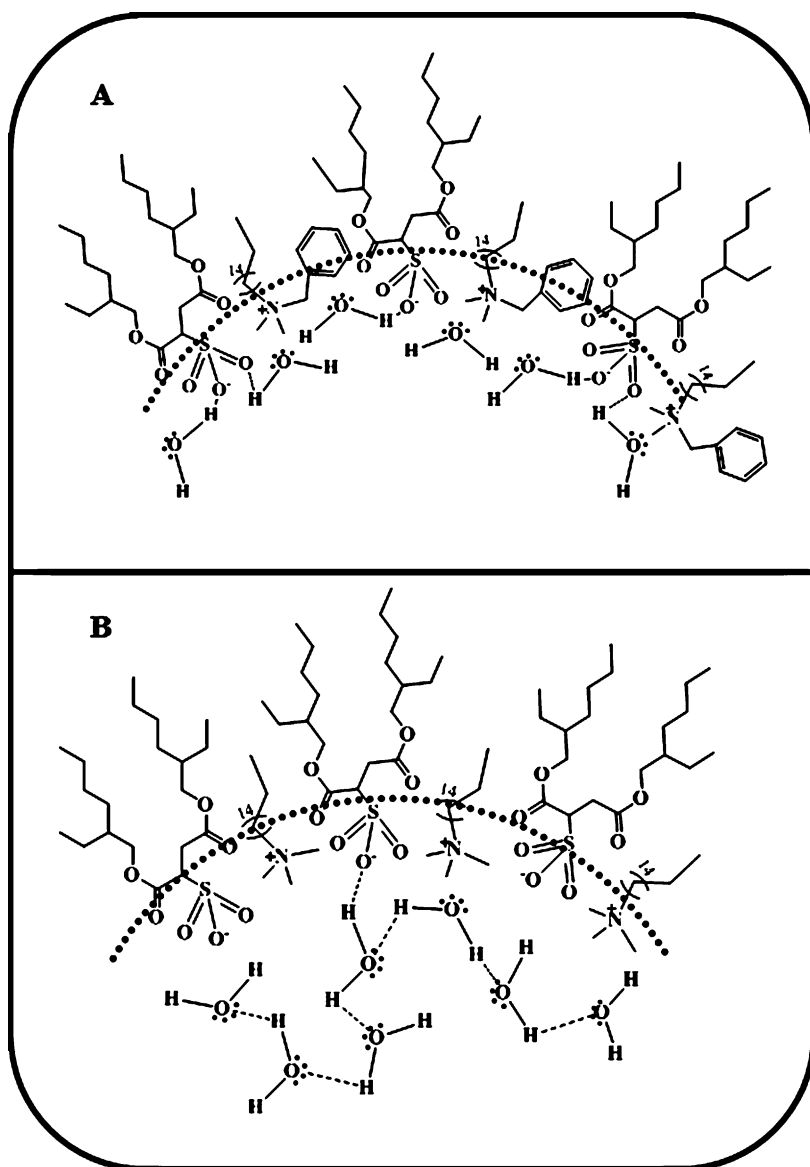


Figure 9. ^1H NMR chemical shifts of $\text{H}\alpha'$ (■) and $\text{H}\beta'$ (●) in benzene/AOT-CTA/water RMs at different W_0 values. [AOT-CTA] = 0.05 M.

nent showed changes in the presence of water because both remained constant across the whole range of W_0 studied. This behavior suggests that the water molecules do not interact with the CTA^+ cation (see Scheme 3B), which emphasizes the idea that the entrapped water in AOT-CTA RMs interacts weakly with the interface, as shown by the DLS and FTIR data.

3. Conclusion

In summary, we created two catanionic surfactants (AOT-BHD and AOT-CTA) formed from traditional ionic surfactants (Na-AOT, BHDC, and CTAB) that are not only ILs but also have amphiphilic properties and can be used to create RMs in nonpolar solvents. In particular, the benzene/AOT-BHD/water and benzene/AOT-CTA/water RMs were investigated by using different noninvasive techniques. The DLS and SLS results revealed the formation of both RMs and that water interacts with the RMs interface because the droplet size increased as the W_0 value was increased. Furthermore, they show that the RMs consist of discrete spherical and noninteracting droplets of water stabilized by the catanionic surfactant. To the best of our knowledge, this is the first report in which AOT-CTA is used to create RMs and encapsulate water. From the FTIR and ^1H NMR spectroscopy data, a difference in the magnitude of the water–catanionic surfactant interaction at the interface was observed. Even though we observed hydrogen-bond interactions with the anionic component for both catanionic surfactants, the strength of this is different for each system. For the AOT-BHD RMs a stronger water–surfactant interaction can be invoked whereas for AOT-CTA this interaction seems to be weaker. This



Scheme 3. Schematic representation of the water molecule distribution in A) AOT-BHD and B) AOT-CTA RMs.

would lead to more water molecules interacting with the interface in AOT-BHD RMs and completely disrupts the hydrogen-bond network of water. Conversely, for AOT-CTA RMs a weaker water–catanionic surfactant interaction allows the water molecules to form hydrogen bonds with each other. We hypothesize that the benzyl group present in the BHD⁺ moiety in AOT-BHD has a notable impact on the behavior of the catanionic interface in comparison with the interface created in AOT-CTA. These results are interesting because a simple change in the cationic component in the catanionic surfactant promotes remarkable changes in the RM interface. In this sense, understanding the structure of water entrapped in RMs is of great importance in many contexts, for example, dehydration of biological molecules,^[57,58] enzyme activity,^[26] water entrapped in nanoporous materials,^[59] and nanoparticles synthesis.^[60]

Experimental Section

Materials

Sodium 1,4-bis-2-ethylhexylsulfosuccinate (Na-AOT), cetyltrimethylammonium bromide (CTAB), and benzyl-*n*-hexadecyldimethylammonium chloride (BHDC) were obtained from Sigma (>99% purity) and were used as received. All surfactants were dried under vacuum prior to use. Ultrapure water was obtained from Labonco equipment model 90901-01. D₂O, benzene, *n*-heptane, chlorobenzene, dichloromethane, and chloroform were obtained from Sigma (HPLC quality) and were used without further purification.

Preparation of Catanionic IL-Like Surfactants

The catanionic IL-like surfactants used, benzyl-*n*-hexadecyldimethylammonium 1,4-bis-2-ethylhexylsulfosuccinate (AOT-BHD, Scheme 1) and cetyltrimethylammonium 1,4-bis-2-ethylhexylsulfosuccinate (AOT-CTA, Scheme 1), were obtained through a modification of a method reported in reference [11]. To obtain AOT-BHD, a mixture of Na-AOT/dichloromethane and BHDC/dichloromethane solutions (containing equimolar fractions of both surfactants) were combined in a round-bottom flask and stirred at RT for 72 h. During the stirring, a white precipitate appeared and was attributed to NaCl formed from the original surfactant counterions. The majority of NaCl was removed from the dichloromethane solution by centrifugation. The dichloromethane solution that contained AOT-BHD was then washed with small amounts of water until the aqueous fraction was free of chloride ion (AgNO₃ test). Once the NaCl was eliminated, the dichloromethane was removed by vacuum evaporation. After isolation, the crude AOT-BHD was further purified by mixing it with activated charcoal and filtering it through a plug of neutral alumina into a round-bottom flask, then drying it under vacuum and storing it under dry nitrogen. The IL (AOT-BHD) was obtained as a colorless and highly viscous liquid, as previously reported.^[15] The same method was used for the synthesis of AOT-CTA, but in this case chloroform was used as the solvent to prepare solutions that contained equimolar fractions of Na-AOT and CTAB. The new surfactant obtained, AOT-CTA, was an amorphous white solid with a melting point of 67 °C, a property that makes it an IL. The formation of both catanionic IL-like surfactants was confirmed by ¹H NMR spectroscopy techniques. Figures S9 and S10 show that all protons corresponding to Na-AOT, BHDC, and CTAB are present. The chemical shifts of AOT-BHD and AOT-CTA obtained in CDCl₃

are included in Tables S1 and S2, respectively, in the Supporting Information. Significant changes in the catanionic surfactants with respect to the chemical shifts of the precursor surfactants were observed (See Tables S1 and S2 in the Supporting Information). These shifts can be attributed to the formation of the catanionic couple. Prior to use, AOT-BHD and AOT-CTA were dried under vacuum for 4 h.

Methods

RM Preparation: Stock solutions of AOT-BHD and AOT-CTA in benzene were prepared by mass and volumetric dilution. Aliquots of these stock solutions were used to make individual solutions of reverse micelles with different amounts of water, defined as $W_0 = [\text{water}]/[\text{surfactant}]$. The incorporation of water into each micellar solution was performed by using calibrated microsyringes. To obtain optically clear solutions, they were shaken in a sonication bath. The resulting solutions were clear solutions with a single phase. The W_0 value was varied between 0–1.6 for AOT-BHD RMs and 0–2.0 for AOT-CTA RMs. It was not possible to obtain higher values of W_0 due to turbidity problems. The lowest value for W_0 ($W_0=0$) corresponds to a system with no added water. In all cases, the catanionic surfactant concentration was kept constant and equal to 0.02 M for the DLS experiments and 0.05 M to the FTIR and NMR experiments.

To evaluate the amount of water (W_0^{max}) able to be dispersed in the systems investigated, we prepared stock solutions of different catanionic concentration (0.02, 0.05, and 0.1 M) in nonpolar solvents (*n*-heptane, chlorobenzene, and benzene) and added water to the samples. The maximum W_0 values reached (W_0^{max}) for both catanionic surfactants were independent of the surfactant concentration.

General

The apparent diameters of the different AOT-BHD and AOT-CTA RMs were determined by dynamic light scattering (DLS, Malvern 4700 with goniometer) with an argon-ion laser operating at $\lambda = 488$ nm. The cleanliness of the cuvettes used for measurements was of crucial importance for obtaining reliable and reproducible data.^[61] Cuvettes were washed with ethanol, then with doubly distilled water, and then dried with acetone. Prior to use the samples were filtered three times by using an Acrodisc with 0.2 μm PTFE membrane (Sigma) to avoid the presence of dust or particles in the original solution. Before introducing each sample to the cuvette, it was rinsed with pure benzene twice, then with the surfactant stock solution, and finally with the sample to be analyzed. Prior making measurements on a given day, the background signals from air and benzene were collected to confirm the cleanliness of the cuvettes. Prior to data acquisition, the samples were equilibrated in the DLS instrument for 10 min at 35 °C. To obtain valid results from the DLS measurements requires knowledge of the system refractive index and viscosity in addition to well-defined conditions. Because we worked with dilute solutions, the refractive indices and viscosities for the RM solutions were assumed to be the same as neat benzene.^[62] Multiple samples at each size were made, and thirty independent size measurements were made for each individual sample at a scattering angle of 90°. The instrument was calibrated before and during the course of the experiments by using several different size standards. Thus, we are confident that the magnitudes obtained by using DLS measurements can be taken as statistically meaningful for all the systems investigated. The algorithm used was CONTIN and the DLS experiments

shown that the polydispersity of the catanionic RMs were less than 5%.

The aggregation numbers (N_{agg}) of the AOT-BHD and AOT-CTA RMs were determined by using a static light scattering (SLS) technique in the same equipment used for the DLS studies. All the measurements were made at an angle of 90° and Debye plots were created by using solutions with different surfactant concentration at a fixed W_0 value for all the RMs studied. From the SLS experiments, the weight-averaged molar masses were determined and the N_{agg} values for all the systems investigated were calculated according to the procedure detailed in literature.^[63] To obtain the dn/dc values (data required for the SLS measurements), a differential refractometer was used (Brookhaven Instruments Corporation, BI-DNDCW model) with a tungsten lamp operating at $\lambda = 470$ nm.

FTIR spectra were recorded by using a Nicolet IMPACT400 FTIR spectrometer. An IR cell of the type Irtan-2 (0.5 mm path length) from Wilmad Glass (Buena, NJ) was used. FTIR spectra were obtained by co-adding 200 spectra at a resolution of 0.5 cm^{-1} . For the experiments performed on C=O and asymmetric SO_3^- stretching modes, the benzene spectrum was used as the background; a different procedure was performed for the O–D stretching band. The $\nu_{\text{O–D}}$ spectral band of HOD was superimposed on a finite background. It was assumed that this background could be approximated with the spectrum of 100% H_2O in the $\nu_{\text{O–D}}$ spectral region.^[44,45,52] Therefore, the reference sample at each W_0 value was a surfactant solution containing exactly the same W_0 but adjusted with pure water. The reason for using partially deuterated water has been explained in the Results and Discussion section.

For the ^1H NMR spectroscopy experiments, a Bruker 400 NMR spectrometer was used. The spectra were recorded at a digital resolution of 0.06 Hz per data point. The spectrometer probe temperature (35 °C) was periodically monitored by measuring the chemical shift difference values between the two singlets of a methanol reference sample which is known to depend on the temperature.^[31] The probe thermal stability was assured by the observation that successive measurements of the sample chemical shift (after 10 min in the probe for thermal equilibration) were within digital resolution limit. For the study on RMs, a capillary tube containing D_2O was introduced in the NMR tube and was used as a frequency “lock”. Chemical shifts were measured relative to internal TMS and the values were reproducible within $\delta = 0.01$ ppm. All NMR spectroscopy data were processed by using MestReC 4.8.6 for Windows and plotted and fitted by using Microcal OriginPro 7 (<http://www.originlab.com/>)

Supporting Information

The SI contains Table S1: ^1H NMR chemical shifts [ppm] for BHDC, Na-AOT, and AOT-BHD surfactants in CDCl_3 ; Table S2: ^1H NMR chemical shifts [ppm] for CTAB, Na-AOT and, AOT-CTA surfactants in CDCl_3 ; Figure S1: FTIR spectra of HDO entrapped in A) benzene/AOT-BHD RMs and B) benzene/AOT-CTA RMs at different W_0 values in the region of 2640–2420 cm^{-1} ($\nu_{\text{O–D}}$); Figure S2: Shifts in the O–D stretching band ($\nu_{\text{O–D}}$) with increasing W_0 for benzene/BHDC/HDO and benzene/Na-AOT/HDO RMs; Figure S3: FTIR spectra of A) benzene/AOT-CTA/water and B) benzene/AOT-BHD/water RMs at different W_0 values in the region of 1700–1770 cm^{-1} ($\nu_{\text{C=O}}$); Figure S4: FTIR spectra of water entrapped in benzene/AOT-BHD RMs at different W_0 values in the region of 1330–1110 cm^{-1} ($\nu_{\text{S}_2\text{O}_3}$); Figure S5: ^1H NMR spectra collected for benzene/AOT-CTA/water RMs at different W_0 values; Figure S6: ^1H NMR chemical shifts of the protons associated with the AOT anion in benzene/AOT-BHD/water

RMs at different W_0 values; Figure S7: ^1H NMR chemical shifts of the protons associated with the anion AOT in benzene/AOT-CTA/water RMs at different W_0 values; Figure S8: ^1H NMR chemical shifts of H β and H γ in benzene/AOT-BHD/water RMs at different W_0 values; Figure S9: ^1H NMR spectrum of AOT-BHD in Cl_3CD ; and Figure S10: ^1H NMR spectrum of AOT-CTA in Cl_3CD .

Acknowledgements

We gratefully acknowledge financial support of this work by the Consejo Nacional de Investigaciones Científicas y Técnicas (CONICET), Agencia Nacional de Promoción Científica y Técnica, and Secretaría de Ciencia y Técnica de la Universidad Nacional de Río Cuarto. J.J.S., N.M.C., and R.D.F. hold a research position at CONICET. C.C.V. thanks CONICET for a research fellowship.

Keywords: catanionic surfactants · ionic liquids · micelles · vibrational spectroscopy · water chemistry

- [1] N. M. Correa, J. J. Silber, R. E. Riter, N. E. Levinger, *Chem. Rev.* **2012**, *112*, 4569–4602.
- [2] R. McNeil, J. K. Thomas, *J. Colloid Interface Sci.* **1981**, *83*, 57–61.
- [3] D. Blach, N. M. Correa, J. J. Silber, R. D. Falcone, *J. Colloid Interface Sci.* **2011**, *355*, 124–130.
- [4] F. M. Agazzi, R. D. Falcone, J. J. Silber, N. M. Correa, *J. Phys. Chem. B* **2011**, *115*, 12076–12084.
- [5] F. M. Agazzi, J. Rodriguez, R. D. Falcone, J. J. Silber, N. M. Correa, *Langmuir* **2013**, *29*, 3556–3566.
- [6] G. Palazzo, F. Lopez, M. Giustini, G. Colafemmina, A. Ceglie, *J. Phys. Chem. B* **2003**, *107*, 1924–1931.
- [7] E. M. Corbeil, N. E. Levinger, *Langmuir* **2003**, *19*, 7264–7270.
- [8] Y. Zhou, W. Lin, H. Wang, Q. Li, J. Huang, M. Du, L. Lin, Y. Gao, L. Lin, N. He, *Langmuir* **2011**, *27*, 166–169.
- [9] S. Sharma, N. Pal, P. K. Chowdhury, S. Sen, A. K. Ganguli, *J. Am. Chem. Soc.* **2012**, *134*, 19677–19684.
- [10] a) K. Yang, L. Z. Zhu, B. S. Xing, *Environ. Sci. Technol.* **2006**, *40*, 4274–4280; b) A. A. Dar, G. M. Rather, S. Ghosh, A. R. Das, *J. Colloid Interface Sci.* **2008**, *322*, 572–581.
- [11] *Specialist Surfactants* (Ed.: I. D. Robb), Blackie Academic and Professional, London, **1997**, pp. 40–41.
- [12] E. W. Kaler, A. K. Murthy, B. Rodriguez, J. A. N. Zasadzinski, *Science* **1989**, *245*, 1371–1374.
- [13] B. F. B. Silva, E. F. Marques, U. Olsson, *Soft Matter* **2011**, *7*, 225–236.
- [14] B. Abécassis, F. Testard, L. Arleth, S. Hansen, I. Grillo, T. Zemb, *Langmuir* **2007**, *23*, 9983–9989.
- [15] C. C. Villa, F. Moyano, M. Ceolin, J. J. Silber, R. D. Falcone, N. M. Correa, *Chem. Eur. J.* **2012**, *18*, 15598–15601.
- [16] a) S. Song, Q. Zheng, A. Song, J. Hao, *Langmuir* **2012**, *28*, 219–226; b) S. Schmölder, D. Gräbner, M. Gradzielski, T. Narayanan, *Phys. Rev. Lett.* **2002**, *88*, 258301; c) X. Li, S. Dong, X. Jia, A. Song, J. Hao, *Chem. Eur. J.* **2007**, *13*, 9495–9502; d) M. Dubois, V. Lizunov, A. Meister, T. Gulik-Krzywicki, J. M. Verbavatz, E. Perez, J. Zimmerberg, T. Zemb, *Proc. Natl. Acad. Sci. USA* **2004**, *101*, 15082–15087; e) J. Hao, W. Liu, G. Xu, L. Zheng, *Langmuir* **2003**, *19*, 10635–10640; f) H. Li, J. Hao, *J. Phys. Chem. B* **2008**, *112*, 10497–10508; g) J. Hao, H. Hoffmann, *Curr. Opin. Colloid Interface Sci.* **2004**, *9*, 279–293.
- [17] B. F. B. Silva, E. F. Marques, U. Olsson, R. Pons, *Langmuir* **2010**, *26*, 3058–3066.
- [18] P. Jokela, B. Jonsson, A. Khan, *J. Phys. Chem.* **1987**, *91*, 3291–3298.
- [19] B. Joansson, P. Jokela, A. Khan, B. Lindman, A. Sadaghiani, *Langmuir* **1991**, *7*, 889–895.
- [20] a) H. Edlund, A. Sadaghiani, A. Khan, *Langmuir* **1997**, *13*, 4953–4963; b) A. González-Pérez, M. Schmutz, G. Waton, M. J. Romero, M. P. Krafft, *J. Am. Chem. Soc.* **2007**, *129*, 756–757; c) Y. W. Shen, J. C. Hao, H. Hoffmann, *Soft Matter* **2007**, *3*, 1407–1412; d) A. Song, S. Dong, X. Jia, J. Hao, W. Liu, T. Liu, *Angew. Chem.* **2005**, *117*, 4086–4089; *Angew. Chem. Int. Ed.* **2005**, *44*, 4018–4021.
- [21] B. F. B. Silva, E. F. Marques, U. Olsson, *Langmuir* **2008**, *24*, 10746–10754.
- [22] B. F. B. Silva, E. F. Marques, U. Olsson, *J. Phys. Chem. B* **2007**, *111*, 13520–13526.
- [23] a) T. Welton, *Green Chem.* **2011**, *13*, 225–225; b) J. P. Hallett, T. Welton, *Chem. Rev.* **2011**, *111*, 3508–3576; c) P. Wasserscheid, W. Keim, *Angew. Chem. Int. Ed.* **2000**, *39*, 3772–3789; d) T. Welton, *Chem. Rev.* **1999**, *99*, 2071–2084; e) T. Welton, P. Wasserscheid, *Ionic Liquids in Synthesis*, Wiley-VCH, Weinheim, **2002**; f) T. Welton, *Coord. Chem. Rev.* **2004**, *248*, 2459–2477.
- [24] a) Y. R. Zhao, X. Chen, B. Jing, X. D. Wang, F. Ma, *J. Phys. Chem. B* **2009**, *113*, 983–988; b) F. Geng, J. Liu, L. Q. Zheng, L. Yu, Z. Li, G. Z. Li, C. H. Tung, *J. Chem. Eng. Data* **2010**, *55*, 147–151.
- [25] a) P. Brown, C. P. Butts, J. Eastoe, D. Fermin, I. Grillo, H.-C. Lee, D. Parker, D. Plana, R. M. Richardson, *Langmuir* **2012**, *28*, 2502–2509; b) P. Brown, C. Butts, R. Dyer, J. Eastoe, I. Grillo, F. Guittard, S. Rogers, R. Heenan, *Langmuir* **2011**, *27*, 4563–4571; c) P. Brown, C. P. Butts, J. Eastoe, I. Grillo, C. James, A. Khan, *J. Colloid Interface Sci.* **2013**, *395*, 185–189.
- [26] F. Moyano, R. D. Falcone, J. C. Mejuto, J. J. Silber, N. M. Correa, *Chem. Eur. J.* **2010**, *16*, 8887–8893.
- [27] S. S. Quintana, R. D. Falcone, J. J. Silber, N. M. Correa, *ChemPhysChem* **2012**, *13*, 115–123.
- [28] A. M. Durantini, R. D. Falcone, J. J. Silber, N. M. Correa, *J. Phys. Chem. B* **2013**, *117*, 3818–3828.
- [29] R. D. Falcone, J. J. Silber, N. M. Correa, *Phys. Chem. Chem. Phys.* **2009**, *11*, 11096–11100.
- [30] T. Liu, Y. Xie, B. Chu, *Langmuir* **2000**, *16*, 9015–9022.
- [31] A. Salabat, J. Eastoe, K. J. Mutch, F. Tabor Rico, *J. Colloid Interface Sci.* **2008**, *318*, 244–251.
- [32] R. A. Day, B. H. Robinson, J. H. R. Clarke, J. V. Doherty, *J. Chem. Soc. Faraday Trans. 1* **1979**, *75*, 132–139.
- [33] A. Maitra, *J. Phys. Chem.* **1984**, *88*, 5122–5125.
- [34] A. Jada, J. Lang, R. Zana, R. Makhloufi, E. Hirsch, S. J. Candau, *J. Phys. Chem.* **1990**, *94*, 381–387.
- [35] D. F. Evans, B. W. Ninham, *J. Phys. Chem.* **1986**, *90*, 226–234.
- [36] Q. Li, T. Li, J. Wu, *J. Colloid Interface Sci.* **2001**, *239*, 522–527.
- [37] D. D. Ferreyra, N. M. Correa, J. J. Silber, R. D. Falcone, *Phys. Chem. Chem. Phys.* **2012**, *14*, 3460–3470.
- [38] D. Blach, J. J. Silber, N. Mariano Correa, R. D. Falcone, *Phys. Chem. Chem. Phys.* **2013**, *15*, 16746–16757.
- [39] N. Gorski, Y. M. Ostanevich, *Ber. Bunsen-Ges.* **1990**, *94*, 737–741.
- [40] A. Jada, J. Lang, R. Zana, R. Makhloufi, E. Hirsch, S. J. Candau, *J. Phys. Chem.* **1990**, *94*, 387–395.
- [41] R. M. Silverstein, F. X. Webster, D. J. Kiemle, *Spectrometric Identification of Organic Compounds*, 7th ed., Wiley, New York, **2005**.
- [42] W. F. Pacynko, J. Yarwood, G. J. T. Tiddy, *Liq. Cryst.* **1987**, *2*, 201–214.
- [43] D. J. Christopher, J. Yarwood, P. S. Belton, B. Hills, *J. Colloid Interface Sci.* **1992**, *152*, 465–472.
- [44] L. P. Novaki, N. M. Correa, J. J. Silber, O. A. El Seoud, *Langmuir* **2000**, *16*, 5573–5578.
- [45] O. A. El Seoud, N. M. Correa, L. P. Novaki, *Langmuir* **2001**, *17*, 1847–1852.
- [46] M. Falk, *J. Chem. Phys.* **1987**, *87*, 28–30.
- [47] P. D. Moran, A. Graham, A. Bowmaker, R. P. Cooney, J. R. Bartlett, J. L. Woolfrey, *Langmuir* **1995**, *11*, 738–743.
- [48] Q. Li, S. Weng, J. Wu, N. Zhou, *J. Phys. Chem. B* **1998**, *102*, 3168–3174.
- [49] G. Calvaruso, A. Minore, V. Turco Liveri, *J. Colloid Interface Sci.* **2001**, *243*, 227–232.
- [50] A. M. Durantini, R. D. Falcone, J. J. Silber, N. M. Correa, *ChemPhysChem* **2009**, *10*, 2034–2040.
- [51] a) T. K. Jain, M. Varshney, A. Maitra, *J. Phys. Chem.* **1989**, *93*, 7409–7416; b) P. D. Moran, G. A. Bowmaker, R. P. Cooney, J. R. Bartlett, J. L. Woolfrey, *J. Mater. Chem.* **1995**, *5*, 295–302.
- [52] N. M. Correa, P. A. R. Pires, J. J. Silber, O. A. El Seoud, *J. Phys. Chem. B* **2005**, *109*, 21209–21219.
- [53] H. Kise, K. Iwamoto, M. Seno, *Bull. Chem. Soc. Jpn.* **1982**, *55*, 3856–3860.
- [54] F. Heatly, *J. Chem. Soc. Faraday Trans. 1* **1988**, *84*, 343–354.
- [55] M. L. Stahla, B. Baruah, D. M. James, M. D. Johnson, N. E. Levinger, D. C. Crans, *Langmuir* **2008**, *24*, 6027–6035.

- [56] R. D. Falcone, B. Baruah, E. Gaidamauskas, C. D. Rithner, N. M. Correa, J. J. Silber, D. C. Crans, N. E. Levinger, *Chem. Eur. J.* **2011**, *17*, 6837–6848.
- [57] a) S. K. Pal, A. H. Zewail, *Chem. Rev.* **2004**, *104*, 2099–2123; b) R. Saha, S. Rakshit, P. K. Verma, R. K. Mitra, S. K. Pal, *J. Mol. Recognit.* **2013**, *26*, 59–66.
- [58] S. Rakshit, R. Saha, S. K. Pal, *J. Phys. Chem. B* **2013**, *117*, 11565–11574.
- [59] A. C. Fogarty, F.-X. Coudert, A. Boutin, D. Laage, *ChemPhysChem* **2014**, *15*, 521–529.
- [60] M. A. López-Quintela, *Curr. Opin. Colloid Interface Sci.* **2003**, *8*, 137–144.
- [61] M. A. Sedgwick, A. M. Trujillo, N. Hendricks, N. E. Levinger, D. C. Crans, *Langmuir* **2011**, *27*, 948–954.
- [62] a) J. P. Blitz, J. L. Fulton, R. D. Smith, *J. Phys. Chem.* **1988**, *92*, 2707–2710; b) H. B. Bohidar, M. Behboudina, *Colloids Surf. A* **2001**, *178*, 313–323.
- [63] C. A. Gracia, S. Gomez-Barreiro, A. Gonzalez-Perez, J. Nimo, J. R. Rodriguez, *J. Colloid Interface Sci.* **2004**, *276*, 408–413.

Received: May 8, 2014

Published online on July 18, 2014